

Reliable wet-chemical cleaning of natively oxidized high-efficiency Cu(In,Ga)Se₂ thin-film solar cell absorbers

Jascha Lehmann, Sebastian Lehmann, Iver Lauermann, Thorsten Rissom, Christian A. Kaufmann, Martha Ch. Lux-Steiner, Marcus Bär, and Sascha Sadewasser

Citation: *Journal of Applied Physics* **116**, 233502 (2014); doi: 10.1063/1.4903976

View online: <http://dx.doi.org/10.1063/1.4903976>

View Table of Contents: <http://scitation.aip.org/content/aip/journal/jap/116/23?ver=pdfcov>

Published by the [AIP Publishing](#)

Articles you may be interested in

[Impact of environmental conditions on the chemical surface properties of Cu\(In,Ga\)\(S,Se\)₂ thin-film solar cell absorbers](#)

J. Appl. Phys. **115**, 183707 (2014); 10.1063/1.4876257

[Intergrain variations of the chemical and electronic surface structure of polycrystalline Cu\(In,Ga\)Se₂ thin-film solar cell absorbers](#)

Appl. Phys. Lett. **101**, 103908 (2012); 10.1063/1.4751261

[Na incorporation into Cu\(In,Ga\)Se₂ thin-film solar cell absorbers deposited on polyimide: Impact on the chemical and electronic surface structure](#)

J. Appl. Phys. **111**, 034903 (2012); 10.1063/1.3679604

[Chemical structure of the \(Zn_{1-x}Mg_x\)O / CuIn\(S,Se\)₂ interface in thin film solar cells](#)

Appl. Phys. Lett. **95**, 122104 (2009); 10.1063/1.3230071




[Chemical and electronic surface structure of 20%-efficient Cu\(In,Ga\)Se₂ thin film solar cell absorbers](#)

Appl. Phys. Lett. **95**, 052106 (2009); 10.1063/1.3194153



AIP | Journal of Applied Physics

Meet The New Deputy Editors

	Christian Brosseau		Laurie McNeil		Simon Phillpot
---	---------------------------	---	----------------------	---	-----------------------

Reliable wet-chemical cleaning of natively oxidized high-efficiency Cu(In,Ga)Se₂ thin-film solar cell absorbers

Jascha Lehmann,^{1,2} Sebastian Lehmann,^{1,3,a)} Iver Laueremann,¹ Thorsten Rissom,¹ Christian A. Kaufmann,¹ Martha Ch. Lux-Steiner,¹ Marcus Bär,^{1,4,b)} and Sascha Sadewasser^{1,5,c)}

¹Renewable Energies, Helmholtz-Zentrum Berlin für Materialien und Energie, Hahn-Meitner-Platz 1, 14109 Berlin, Germany

²Potsdam Institute for Climate Impact Research (PIK), 14473 Potsdam, Germany

³Solid State Physics, Lund University, Box 118, S-22100 Lund, Sweden

⁴Institut für Physik und Chemie, Brandenburgische Technische Universität Cottbus-Senftenberg, Platz der Deutschen Einheit 1, 03046 Cottbus, Germany

⁵International Iberian Nanotechnology Laboratory, Av. Mestre José Veiga s/n, 4715-330 Braga, Portugal

(Received 16 October 2014; accepted 30 November 2014; published online 15 December 2014)

Currently, Cu-containing chalcopyrite-based solar cells provide the highest conversion efficiencies among all thin-film photovoltaic (PV) technologies. They have reached efficiency values above 20%, the same performance level as multi-crystalline silicon-wafer technology that dominates the commercial PV market. Chalcopyrite thin-film heterostructures consist of a layer stack with a variety of interfaces between different materials. It is the chalcopyrite/buffer region (forming the p-n junction), which is of crucial importance and therefore frequently investigated using surface and interface science tools, such as photoelectron spectroscopy and scanning probe microscopy. To ensure comparability and validity of the results, a general preparation guide for “realistic” surfaces of polycrystalline chalcopyrite thin films is highly desirable. We present results on wet-chemical cleaning procedures of polycrystalline Cu(In_{1-x}Ga_x)Se₂ thin films with an average $x = [\text{Ga}]/([\text{In}] + [\text{Ga}]) = 0.29$, which were exposed to ambient conditions for different times. The hence natively oxidized sample surfaces were etched in KCN- or NH₃-based aqueous solutions. By x-ray photoelectron spectroscopy, we find that the KCN treatment results in a chemical surface structure which is – apart from a slight change in surface composition – identical to a pristine as-received sample surface. Additionally, we discover a different oxidation behavior of In and Ga, in agreement with thermodynamic reference data, and we find indications for the segregation and removal of copper selenide surface phases from the polycrystalline material. © 2014 AIP Publishing LLC. [<http://dx.doi.org/10.1063/1.4903976>]

I. INTRODUCTION

Thin-film solar cells based on polycrystalline p-type Cu(In_{1-x}Ga_x)Se₂ absorbers show the highest power conversion efficiencies (>21%)¹ among all thin-film solar cell photovoltaic materials. Typical chalcopyrite solar cells consist of a stack of various semiconductors and metals, consecutively deposited onto glass substrates. In this multilayer architecture, the chemical, structural, and electronic interface properties play a crucial role for the overall performance of the final solar cell device. In this respect, with the goal to improve understanding of the interface formation and properties, and to ultimately improve solar cell efficiencies, a significant number of surface and interface studies have been performed in the past, many of those using photoemission spectroscopy^{2–9} or scanning probe microscopy.^{10–14} The conclusions based on the findings from these techniques mainly rely on the measurement of clean sample surfaces under ultrahigh vacuum (UHV) conditions. However, for such kind of studies, samples are typically obtained from independent growth equipment and are transferred through air into the UHV of the

experimental setup for characterization. Contamination and oxidation can significantly influence the results of these characterization techniques. Therefore, it is important to create reproducible and well defined surfaces with respect to their composition that are free of contamination.

In the past, results on the oxidation of Cu(In_{1-x}Ga_x)Se₂ surfaces and their chemical etching have been presented. It was found that etching in NH₃- and KCN-based solutions can remove undesired secondary phases and oxides from the surface of Cu(In,Ga)(S,Se)₂, as, i.e., Cu-selenides or SeO₂.^{3,15,16} Kazmerski *et al.* studied the oxidation of CuInSe₂ by controlled oxygen exposure under UHV conditions and the subsequent cleaning using ion etching.¹⁵ An oxidation study of CuGaSe₂ was presented by Würz *et al.*,⁶ who compared the oxidation after different exposure times to air. X-ray photoelectron spectroscopy (XPS) was then used to analyze the different oxide phases present at the surface. However, so far, a systematic study of how good wet-chemical surface cleaning procedures work for different degrees of surface oxidation is still missing.

In this paper, we present a study of the native oxidation of polycrystalline Cu(In_{1-x}Ga_x)Se₂ thin films, which were oxidized for different periods of time and subsequently wet-chemically treated in basic solutions (KCN or NH₃).

^{a)}sebastian.lehmann@ftf.lth.se

^{b)}marcus.baer@helmholtz-berlin.de

^{c)}sascha.sadewasser@inl.int

The composition and the degree of oxidation were analyzed using surface sensitive XPS and x-ray excited Auger electron (XAES) spectroscopy. Mg K_{α} and Al K_{α} radiation were used as complementary excitation sources to gain depth-resolved information. The results of our study indicate that a KCN etch provides a chemical surface structure almost identical to a pristine sample surface.

II. EXPERIMENTAL

A. Sample growth

Polycrystalline $\text{CuIn}_{0.71}\text{Ga}_{0.29}\text{Se}_2$ layers were deposited onto Mo-coated soda-lime glass substrates by a well-established multi-stage co-evaporation process.^{17,18} In the first step, In, Ga, and Se are evaporated at a substrate temperature of $T_{\text{sub}} = 330^\circ\text{C}$ resulting in a nominal $(\text{In}_{0.71}\text{Ga}_{0.29})_2\text{Se}_3$ layer composition. During the second step, Cu and Se are deposited at a higher temperature $T_{\text{sub}} = 530^\circ\text{C}$. Once the stoichiometric point is just passed, i.e., $[\text{Cu}]/([\text{In}] + [\text{Ga}]) > 1$, the Cu flux is turned off. In the third step, In, Ga, and Se are evaporated until a slightly Cu-poor sample composition is reached with values of about $[\text{Cu}]/([\text{In}] + [\text{Ga}]) \approx 0.79$.

B. Sample conditioning

To analyze the oxidation behavior of the $\text{CuIn}_{0.71}\text{Ga}_{0.29}\text{Se}_2$ thin films, the samples were exposed for different durations (<3 min, 100 h, 1000 h) to ambient air (19% oxygen, 81% nitrogen). The samples were stored in the dark and kept under relatively constant ambient conditions of 21–23 °C and 20–25% humidity. In the following, these ambient conditions will be simply described as *air-exposed*. The samples with <3 min, 100 h, and 1000 h air exposure will be referred to as “CIGSe 3 min,” “CIGSe 100 h,” and “CIGSe 1000 h,” respectively.

Immediately after the defined air exposure, the surface of each sample was wet-chemically treated using KCN- or NH_3 -based aqueous solutions. The NH_3 treatment consisted of dipping the sample in 1.5 mol/l aqueous NH_3 solution for 10 s, 100 s, or 1000 s at room temperature. This treatment resembles cleaning processes similar to those occurring during the standard wet-chemical CdS buffer deposition. For the KCN treatment, the $\text{CuIn}_{0.71}\text{Ga}_{0.29}\text{Se}_2$ layers were dipped into 0.15 mol/l aqueous KCN solution for 2 min also at room temperature. After the respective treatments, all samples were rinsed with N_2 -purged de-ionized water and subsequently dried with N_2 . The surface treatment of all samples was performed under inert gas atmosphere in a N_2 -filled glovebox with an O_2 concentration of ≤ 1 ppm attached to the UHV chamber of the XPS setup. Therefore, post-cleaning re-exposure of the samples to ambient conditions could be minimized.

C. Measuring and analysis procedure

For the XPS/XAES measurements, Mg K_{α} and Al K_{α} radiation as excitation sources and a CLAM 4 analyzer (VG-Scienta) with a 9-channeltron detector were used, operated in an analysis chamber at a base pressure of 10^{-10} mbar. The calibration of the energy scale was carried out according to

reported methods and reference data.¹⁹ Characteristic photoemission and Auger lines of Ga, In, Cu, and Se were recorded as a function of the sample's air exposure time and surface treatment for further qualitative data analysis.

To gain quantitative information, the different spectral photoemission lines were fitted with Voigt functions and a combination of a linear and Shirley background. Unless otherwise noted, the following general constraints were applied: the full width at half maximum (FWHM), determined for a certain spectral line, was fixed for all fits of this line, which were measured with the same excitation source. Exceptions had to be made for all spectral lines of the “CIGSe 1000 h” sample as the channeltrons of the XPS setup had to be changed after the characterization of the “CIGSe 100 h” samples and prior to these measurements. As a result, the energy resolution of the measurement setup was slightly changed. Both peaks of a spin-orbit doublet were fitted with the identical FWHM and a fixed intensity ratio according to their multiplicity ($2j + 1$).

The line-specific FWHM was determined as follows: For the “CIGSe 3 min” and “CIGSe 100 h” sample, the FWHM was determined from the fit of the KCN-treated “CIGSe 3 min” sample. This procedure presumes that the surface of this sample is most defined, i.e., significant oxide and binary selenide phases are absent, as could be evaluated from the analysis of respective Auger spectra. For the “CIGSe 1000 h” sample, the FWHM was determined analogously from the KCN treated “CIGSe 1000 h” sample. The described procedure was performed for both Al K_{α} and Mg K_{α} excitation. However, as we cannot exclude minor contaminations even after the KCN-treatment of the sample and since the surface of the KCN treated sample does not necessarily have to be completely identical to the initial pristine state of the $\text{CuIn}_{0.71}\text{Ga}_{0.29}\text{Se}_2$ layer directly after the deposition process, this approach is considered to be an approximation. In Sec. III, it will be discussed how good this approach is.

III. RESULTS AND DISCUSSION

A. Qualitative analysis of the oxidation behavior by examination of Auger lines

In the following, we present the qualitative analysis of the element-specific oxidation behavior of the investigated $\text{CuIn}_{0.71}\text{Ga}_{0.29}\text{Se}_2$ films. The Auger lines of the corresponding elements were evaluated in detail for that purpose. Fig. 1 shows the Ga $L_3M_{45}M_{45}$ line taken for all samples and surface treatments. The highest intensity feature observed for all samples (except for the untreated “CIGSe 1000 h” sample) independent of exposure time and wet-chemical treatment at $E_{\text{kin}} = (1065.6 \pm 0.2)$ eV can be assigned to gallium in a chalcopyrite environment.^{2,20} In particular, for the untreated $\text{CuIn}_{0.71}\text{Ga}_{0.29}\text{Se}_2$ samples that have been exposed to air for 100 h and 1000 h a second feature emerging at $E_{\text{kin}} = (1062.2 \pm 0.2)$ eV can be clearly identified. This is indicative for an air-exposure-induced formation of a Ga_2O_3 surface phase as concluded from the good agreement with respective literature values,^{4,21} see corresponding black boxes in Fig. 1. Note that the feature at around 1069 eV kinetic

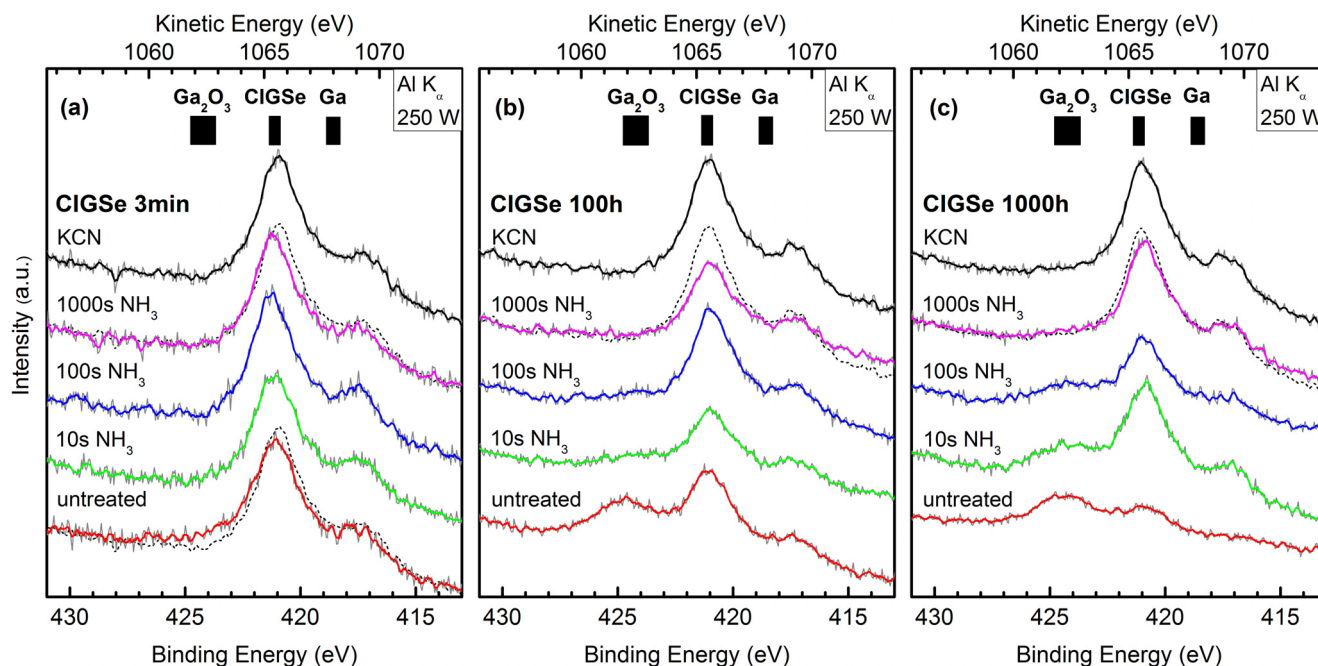


FIG. 1. Ga $L_{3}M_{45}M_{45}$ Auger spectra of the $\text{CuIn}_{0.71}\text{Ga}_{0.29}\text{Se}_2$ (CIGSe) samples exposed to ambient conditions for (a) < 3 min, (b) 100 h, and (c) 1000 h and after different wet chemical surface treatments. The spectra are shifted along the y-axis and given as raw (gray) and smoothed (colored) lines for clarity. The black boxes indicated at the top correspond to reference positions of related compounds taken from literature.^{2,4,20,21} The detailed spectrum of the respective KCN-treated sample (black dotted line) is overlaid with selected individual spectra for direct comparison.

energy, visible in most of the spectra, belongs to the Ga $L_{3}M_{45}M_{45}$ Auger spectrum of gallium in a chalcopyrite environment and is not indicative for the presence of metallic Ga. Increasing the air-exposure time results in an intensity increase in the Ga $L_{3}M_{45}M_{45}$ feature attributed to Ga_2O_3 . Note that close inspection of the untreated “CIGSe 3 min” spectrum—in particular, in direct comparison with the respective KCN etched sample in Fig. 1(a)—reveals that Ga_2O_3 traces might even be present on that sample, i.e., 3 min of air exposure is sufficient for the oxidation of gallium. Thus, even the direct and fast transfer of the sample and a minimized air-exposure could not prevent a partial oxidation of the gallium present at the $\text{CuIn}_{0.71}\text{Ga}_{0.29}\text{Se}_2$ surface. However, it can be observed that all wet-chemical treatments are well-suited to completely remove the Ga_2O_3 phase from the 3 min air-exposed sample surfaces. This is in contrast to the situation for the 100 h and 1000 h air-exposed samples. Here, only the 1000 s NH_3 and the KCN treatment resulted in a complete removal of the Ga_2O_3 phase.

Next, we focus on the analysis of the chemical environment of indium present at the surface of the $\text{CuIn}_{0.71}\text{Ga}_{0.29}\text{Se}_2$ absorber and how it changes upon air exposure and subsequent wet-chemical treatments. Fig. 2 shows the spectral region of the In $M_{45}N_{45}N_{45}$ Auger and Na 1s photoemission line of the $\text{CuIn}_{0.71}\text{Ga}_{0.29}\text{Se}_2$ samples exposed to ambient conditions and after different wet chemical surface treatments. The In $M_{45}N_{45}N_{45}$ Auger peak at $E_{\text{kin}} = (408.0 \pm 0.2)$ eV is indicative for indium being in a chemical chalcopyrite environment.^{2,20} Note that the shoulder at around 410 eV kinetic energy belongs to the In $M_{45}N_{45}N_{45}$ Auger spectrum of indium in a chalcopyrite environment and is not indicative for the presence of metallic In. However, similarly to gallium, we also find evidence for the oxidation of the indium for the

$\text{CuIn}_{0.71}\text{Ga}_{0.29}\text{Se}_2$ layers that have been exposed to air for 100 h and 1000 h. The first indication for the presence of a second indium species is the increase in spectral intensity that fills the dip in-between the In $M_{45}N_{45}N_{45}$ and the In $M_{55}N_{45}N_{45}$ Auger features at $E_{\text{kin}} \approx 405$ eV and the formation of a shoulder at $E_{\text{kin}} \approx 397.5$ eV. This results in an overall broadening of the Auger spectrum. For the “CIGSe 1000 h” samples in Fig. 2(c), even the appearance of an additional In $M_{45}N_{45}N_{45}$ Auger line at a kinetic energy of $E_{\text{kin}} = (406.5 \pm 0.2)$ eV can be observed, which can be attributed to In_2O_3 , concluded from the good agreement with respective literature values^{22,23} (see corresponding black boxes in Fig. 2). Note that the direct spectral comparison of the KCN-etched with the untreated “CIGSe 3 min” sample does not indicate a significant presence of In_2O_3 on the absorber surface. In contrast to the wet-chemical removal of Ga_2O_3 from the $\text{CuIn}_{0.71}\text{Ga}_{0.29}\text{Se}_2$ surface discussed above, the surface indium oxide can only be completely removed from the “CIGSe 100 h” sample by the 1000 s NH_3 and the KCN treatments but not—by any treatment—from the “CIGSe 1000 h” sample. This is clearly indicated by the pronounced shoulder at $E_{\text{kin}} \approx 397$ eV and the additional spectral intensity at $E_{\text{kin}} \approx 406$ eV when comparing the spectra of the KCN etched “CIGSe 1000 h” (top spectrum in Fig. 2(c)) and the KCN-etched “CIGSe 3 min” (top spectrum in Fig. 2(a)) samples. Reasons for why the 1000 s NH_3 and the KCN treatments are able to remove the oxidized indium from the “CIGSe 100 h” but not from the “CIGSe 1000 h” sample could be the formation of different indium oxides (that are more or less soluble) and/or different oxide thicknesses.

Furthermore, Na 1s photoemission peaks can be observed for all untreated $\text{CuIn}_{0.71}\text{Ga}_{0.29}\text{Se}_2$ layers. The sodium stems from the employed soda-lime glass substrate. It is well known that at the elevated temperatures, during

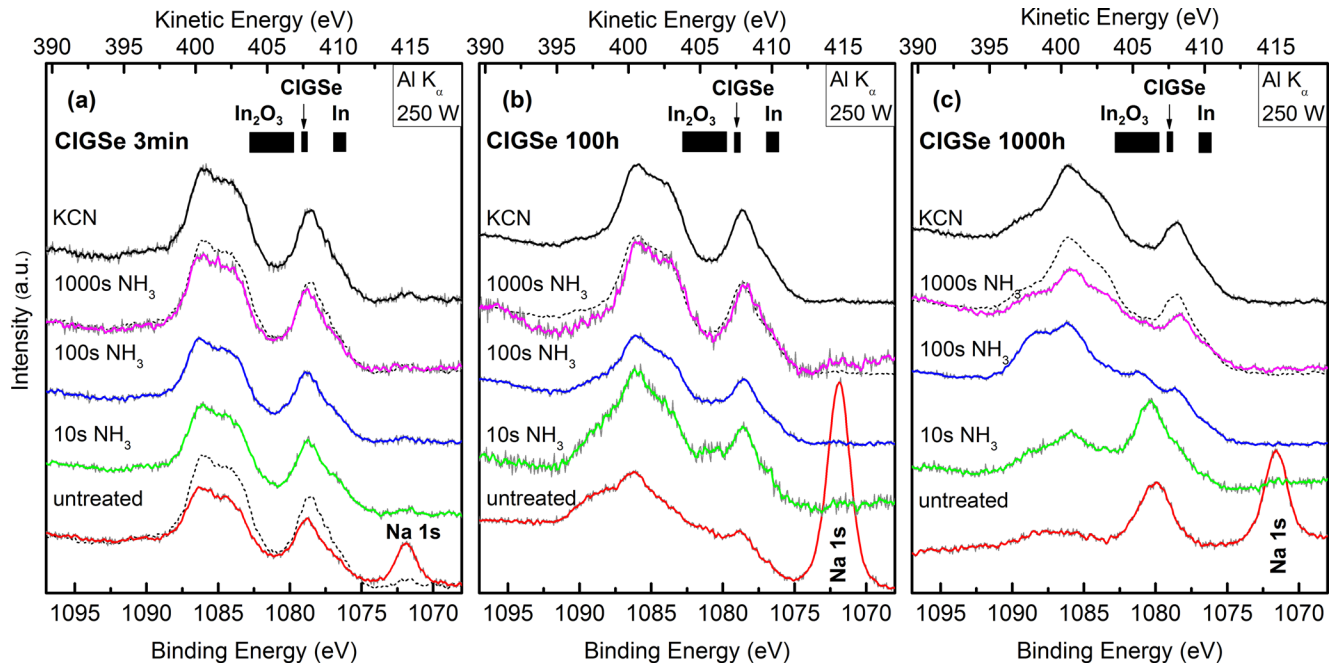


FIG. 2. Spectral region of the In $M_{45}N_{45}N_{45}$ Auger and Na 1s photoemission line of the $\text{CuIn}_{0.71}\text{Ga}_{0.29}\text{Se}_2$ (CIGSe) samples exposed to ambient conditions for (a) < 3 min, (b) 100 h, and (c) 1000 h and after different wet chemical surface treatments. The spectra are shifted along the y-axis and given as raw (gray) and smoothed (colored) lines for clarity. The black boxes indicated at the top correspond to In $M_{45}N_{45}N_{45}$ reference positions of related compounds taken from literature.^{2,20,22,23} The detailed spectrum of the respective KCN-treated sample (black dotted line) is overlaid with selected individual spectra for direct comparison.

absorber formation, sodium diffuses through the Mo back contact and the chalcopyrite layer and accumulates at the surface.²⁴ Apparently, the sodium is removed by all wet-chemical treatments from the $\text{CuIn}_{0.71}\text{Ga}_{0.29}\text{Se}_2$ surface, a finding that was reported by several groups before.^{25,26}

Next, we are addressing how the chemical environment of the selenium at the surface of the $\text{CuIn}_{0.71}\text{Ga}_{0.29}\text{Se}_2$ layer

changes upon air exposure and subsequent wet-chemical treatments. The respective Se $L_{3M_{45}M_{45}}$ Auger line of the $\text{CuIn}_{0.71}\text{Ga}_{0.29}\text{Se}_2$ samples exposed to ambient conditions and after different wet chemical surface treatments is shown in Fig. 3. The Se $L_{3M_{45}M_{45}}$ Auger peak at $E_{\text{kin}} = (1307.3 \pm 0.2)$ eV is indicative for selenium being in a chemical chalcopyrite environment.^{2,20} Selenium oxidation occurs on a larger time

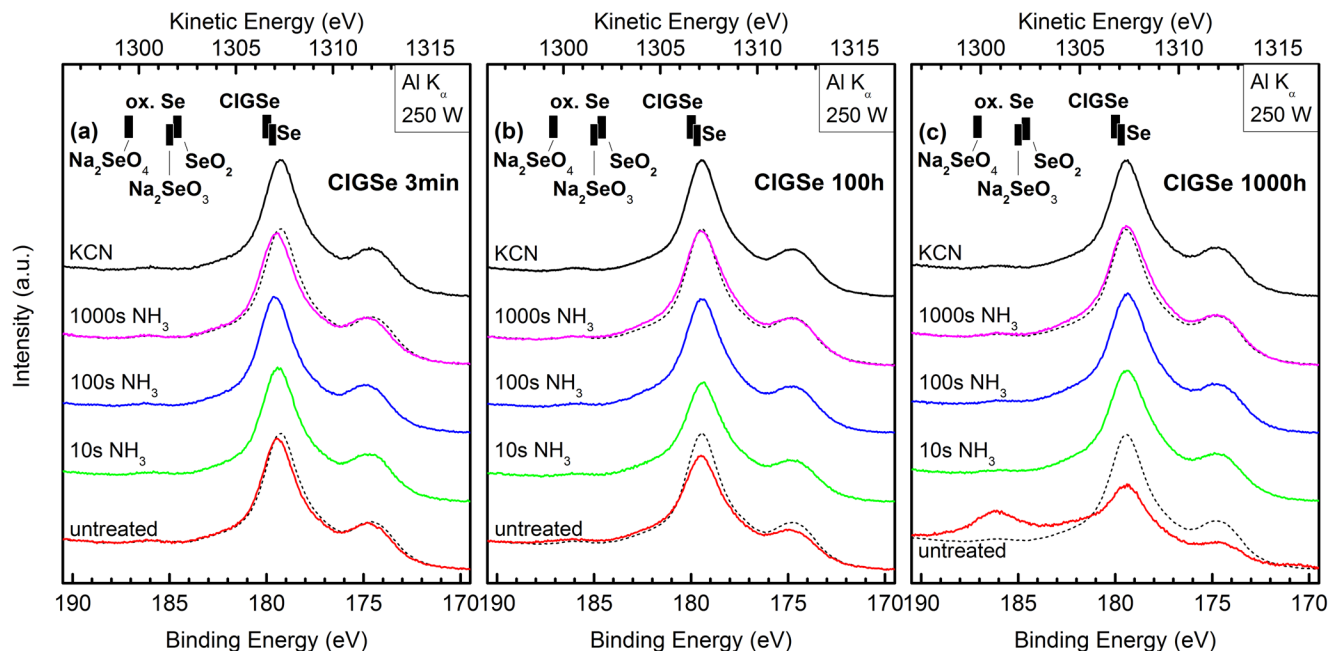


FIG. 3. Se $L_{3M_{45}M_{45}}$ Auger line of the $\text{CuIn}_{0.71}\text{Ga}_{0.29}\text{Se}_2$ (CIGSe) samples exposed to ambient conditions for (a) < 3 min, (b) 100 h, and (c) 1000 h and after different wet chemical surface treatments. The spectra are shifted along the y-axis for clarity. The black boxes indicated at the top correspond to reference positions of related compounds taken from literature.^{2,20,27,28} The detailed spectrum of the respective KCN-treated sample (black dotted line) is overlaid with selected individual spectra for direct comparison.

scale when compared to the previously discussed surface oxidation of gallium and indium. A feature at a kinetic energy of $E_{\text{kin}} = (1300.4 \pm 0.2)$ eV, which is attributed to an oxidized Se phase, is not observed in significant intensity until 1000 h of air exposure (Fig. 3(c)). Note that the derived energy positions of the measured Se $L_3M_{45}M_{45}$ Auger spectra slightly deviate from the reported kinetic energies for selenium being in a chalcopyrite environment (represented as black box in Fig. 3), which is attributed to the limited Se $L_3M_{45}M_{45}$ reference data available in literature resulting in significantly smaller energy ranges, indicating the spread of literature positions for selenium compounds. In consequence, the Se $L_3M_{45}M_{45}$ energy ranges are much narrower compared to those given for gallium and indium species (compare dimensions of black boxes in Figs. 1–3) which might be the reason for the observed slight deviation. Thus, the comparison of the experimentally derived kinetic energy of the oxidized Se phase feature with reference positions of potentially formed Se- O_x species from Refs. 27 and 28 (indicated as “ox. Se” in Fig. 3) is not as straightforward as the narrow reference positions might promise and so an identification of the oxidized Se phase is not attempted. However, for untreated samples (see also Fig. 2), the presence/formation of a Na-Se- O_x species cannot be excluded. In any case, all wet-chemical treatments remove the oxidized Se phase from the “CIGSe 1000 h” sample (see Fig. 3(c)).

Comparing the Cu $L_3M_{45}M_{45}$ Auger spectra (not shown) of the $\text{CuIn}_{0.71}\text{Ga}_{0.29}\text{Se}_2$ layers for different air exposure times and wet-chemical treatments revealed no significant spectral changes and thus no indications for a surface oxidation of copper could be observed. Note that this conclusion might be corrupted as the difference in the kinetic energies of the Cu $L_3M_{45}M_{45}$ Auger line for different copper compounds is smaller than the FWHM of the Auger line itself.

See Cu 2p data discussion related to Fig. 7 for more insights into the chemical environment of Cu.

B. Quantitative analysis of the surface composition

Quantitative analysis of the surface composition was obtained from fits of specific photoemission lines of the involved elements. In the following, we present the analysis for each element in the sequence as presented for the qualitative analysis above. The surface content of gallium was analyzed using the Ga $2p_{3/2}$ photoemission line (see Fig. 4). As a result of the already discussed presence of Ga_2O_3 at the $\text{CuIn}_{0.71}\text{Ga}_{0.29}\text{Se}_2$ surface (see above), an asymmetric broadening of the peak towards higher binding energies is expected and can be observed—least prominent for the untreated samples and increasing with air exposure time. Hence, the Ga $2p_{3/2}$ line was fitted by two Voigt functions. Fig. 4 shows the experimental data and the fits of the Ga $2p_{3/2}$ line as a function of the samples exposure time to air and chemical surface treatment.

The difference in the binding energy between the chalcopyrite and Ga_2O_3 contribution to the Ga $2p_{3/2}$ line was derived for the untreated “CIGSe 1000 h” sample, i.e., the sample with the highest degree of surface oxidation, to be $\Delta E = 0.95$ eV. This binding energy difference was restrained for all fits. Furthermore, the derived binding energies of the Ga $2p_{3/2}$ components for chalcopyrite [$E_B(\text{CIGSe}) = (1117.6 \pm 0.1)$ eV] and Ga_2O_3 [$E_B(\text{Ga}_2\text{O}_3) = (1118.7 \pm 0.1)$ eV], respectively, are also in good agreement with reported literature values.^{2,20,21} The wet-chemical treatments result in a decrease in the Ga_2O_3 contribution and thus a more symmetric Ga $2p_{3/2}$ line shape. In agreement with the qualitative observations based on the Ga $L_3M_{45}M_{45}$ Auger spectra in Fig. 1, also the Ga $2p_{3/2}$ XPS data indicate that the longer the air-exposure time and thus the

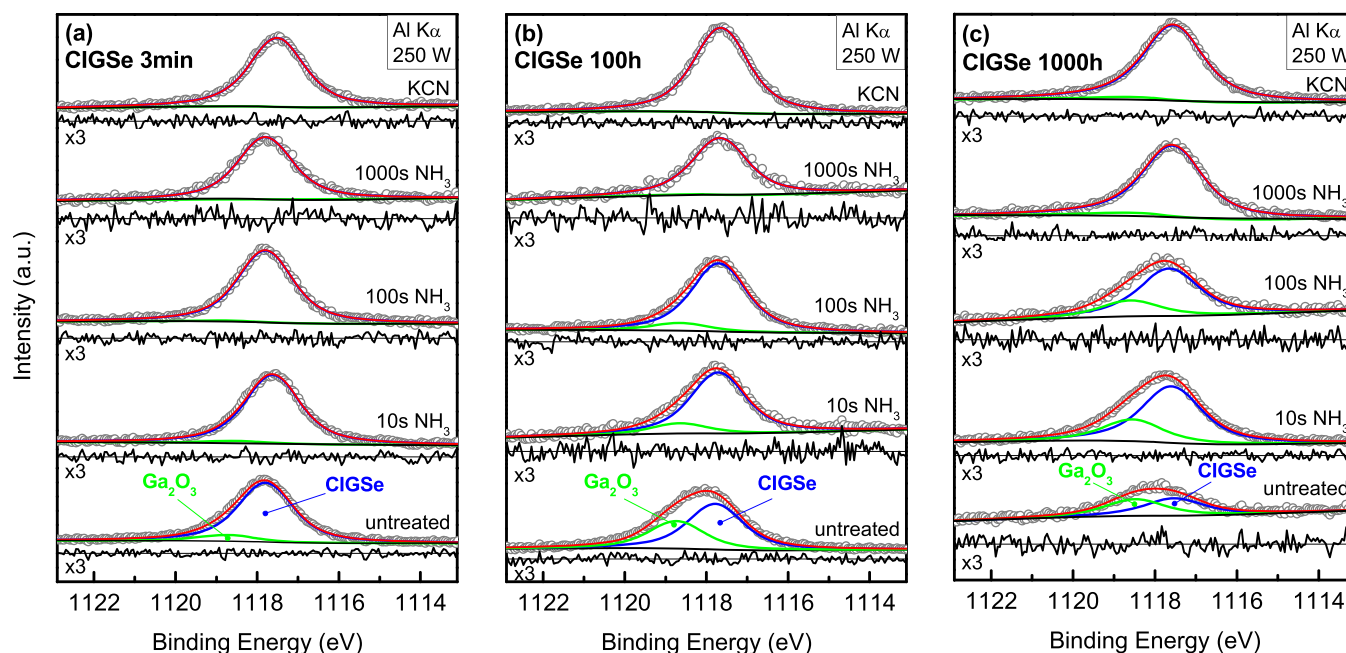


FIG. 4. Ga $2p_{3/2}$ photoemission spectra (Al K_{α} excitation) of the $\text{CuIn}_{0.71}\text{Ga}_{0.29}\text{Se}_2$ (CIGSe) samples exposed to ambient conditions for (a) < 3 min, (b) 100 h, and (c) 1000 h and after different wet chemical surface treatments. Experimental data (open circles) are shown together with respective fits of the CIGSe component (blue line), a Ga_2O_3 component (green line), and the sum of both (red line). Voigt profiles together with a combined Shirley and linear background (black line below each detail spectrum) were used for the simultaneously performed fits. Below each spectrum, the magnified residual ($\times 3$) of the fit is shown.

higher the resulting degree of surface gallium oxidation, the longer the $\text{CuIn}_{0.71}\text{Ga}_{0.29}\text{Se}_2$ sample needs to be treated in NH_3 to remove the Ga_2O_3 completely. In particular, for the “CIGSe 3 min” sample 10 s and for the “CIGSe 1000 h” samples 1000 s of NH_3 treatment is necessary. The KCN treatment also completely removes the surface gallium oxides from the $\text{CuIn}_{0.71}\text{Ga}_{0.29}\text{Se}_2$ samples.

Next, we address the quantification of the formation of surface indium oxide on the air-exposed $\text{CuIn}_{0.71}\text{Ga}_{0.29}\text{Se}_2$ surface. The corresponding $\text{In } 3d_{3/2}$ photoemission lines are shown for all air-exposure times and wet-chemical treatments in Fig. 5. Similarly to the $\text{Ga } 2p_{3/2}$ photoemission line, also for the $\text{In } 3d_{3/2}$ peak, we find an increased asymmetry towards higher binding energies with increased air exposure time. Hence, also the $\text{In } 3d_{3/2}$ line was fitted with two Voigt functions. The main contribution was found to be at $E_B = (452.2 \pm 0.1)$ eV and attributed to indium in a chalcopyrite environment. The component at higher binding energy $E_B = (453.0 \pm 0.1)$ eV was ascribed to In_2O_3 . Both, the derived binding energy positions as well as the binding energy difference $\Delta E = 0.8$ eV are in agreement with literature values for chalcopyrites and In_2O_3 .¹⁵ The derived increasing In_2O_3 contribution to the $\text{In } 3d_{3/2}$ photoemission line with increasing air exposure time confirms the above formulated observation of a more pronounced peak asymmetry. Again in agreement with the more qualitative assessment of the surface indium oxidation based on the $\text{In } M_{45}N_{45}N_{45}$ Auger spectra shown in Fig. 2, the $\text{In } 3d_{3/2}$ XPS data indicate the complete removal of the surface oxide from the “CIGSe 100 h” sample by the 1000 s NH_3 and KCN treatment but not—by any treatment—from the “CIGSe 1000 h” sample.

The degree of surface selenium oxidation through air exposure was quantified based on the corresponding $\text{Se } 3d$ XPS

data shown in Fig. 6 for all exposure times and wet-chemical treatments. For the “CIGSe 100 h” and “CIGSe 1000 h” samples, again an asymmetry of the photoemission line towards higher binding energies can be observed. This is, however, less pronounced than for the $\text{Ga } 2p_{3/2}$ and $\text{In } 3d_{3/2}$ peaks discussed above. Furthermore, this asymmetry does not increase when comparing the 100 h to 1000 h air exposure samples. This qualitative observation is confirmed by the fit of the $\text{Se } 3d$ spectra using two doublets. The first (most prominent) doublet is located at a binding energy of $E_B(3d_{5/2}/3d_{3/2}) = (54.0/54.9 \pm 0.1)$ eV, which is characteristic for selenium in a chalcopyrite chemical environment.^{2,6} Note that for the fits of the $3d_{5/2}/3d_{3/2}$ peak, the spin-orbit separation of the doublet was derived from the KCN treated “CIGSe 3 min” sample to be $\Delta E_B = (0.8 \pm 0.1)$ eV first and then restrained for all fits. To account for the line asymmetry observed for the “CIGSe 100 h” and “CIGSe 1000 h” samples, a second $\text{Se } 3d$ doublet was fitted at $E_B(3d_{5/2}/3d_{3/2}) = (54.9/55.8 \pm 0.1)$ eV. According to literature,¹⁵ this second doublet could be attributed to selenium in a partially oxidized environment or to a Cu_{2-x}Se compound. However, as this second doublet does not disappear upon (even extended) treatment in aqueous NH_3 solution but completely vanishes after the KCN treatment,²⁹ we tentatively ascribe it to be indicative for the presence of Cu_{2-x}Se at the “CIGSe 100 h” and “CIGSe 1000 h” samples surface.

In agreement with the qualitative assessment based on the $\text{Se } L_3M_{45}M_{45}$ in Fig. 3, which only revealed a significant selenium oxidation for the untreated “CIGSe 1000 h” sample, we find a significant high-binding energy contribution to the $\text{Se } 3d$ line at a binding energy of $E_B(3d_{5/2}/3d_{3/2}) = (59.0/59.9 \pm 0.1)$ eV—in agreement with the $\text{Se } 3d$ (SeO_2) binding energy position reported in Refs. 15 and 28—only for the

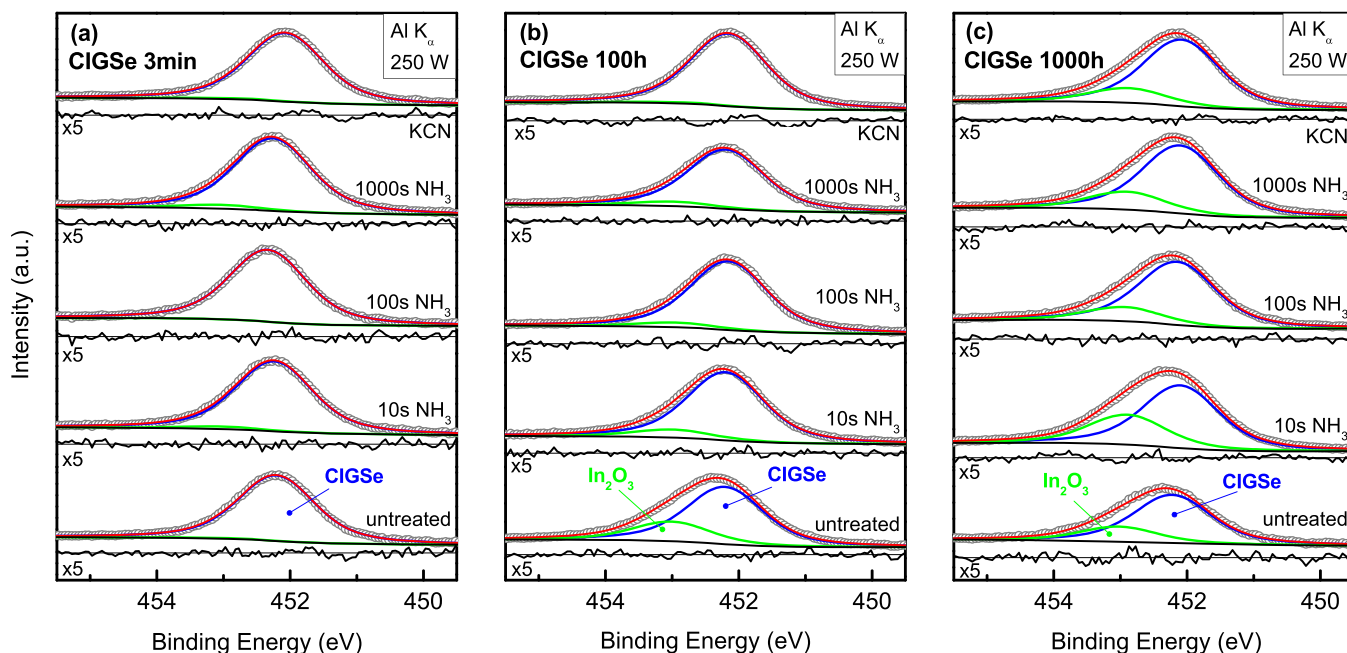


FIG. 5. $\text{In } 3d_{3/2}$ photoemission spectra ($\text{Al } K_\alpha$ excitation) of $\text{CuIn}_{0.71}\text{Ga}_{0.29}\text{Se}_2$ (CIGSe) samples exposed to air for (a) < 3 min, (b) 100 h, and (c) 1000 h and after different wet chemical surface treatments. Experimental data (open circles) are shown together with respective fits of the CIGSe component (blue line), an In_2O_3 component (green line), and the sum of both (red line). Voigt profiles together with a combined Shirley and linear background (black line below each detail spectrum) were used for the simultaneously performed fits. Below each spectrum the magnified residual ($\times 5$) of the fit is shown.

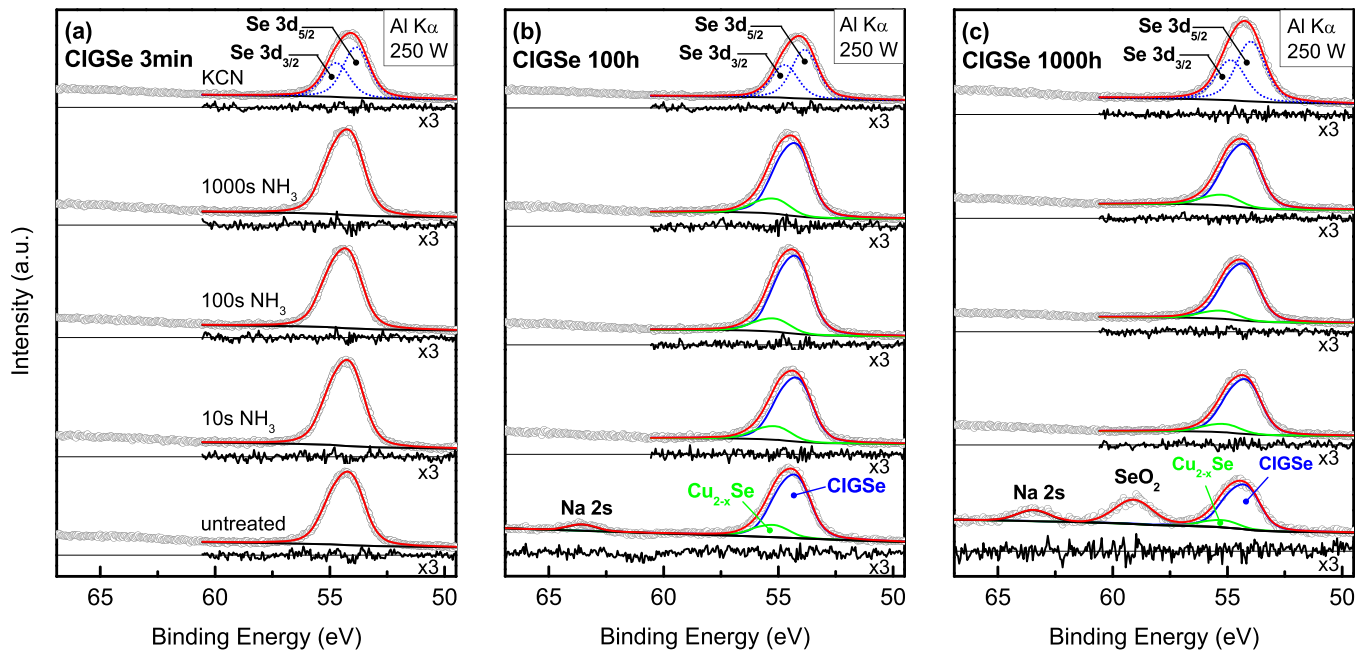


FIG. 6. Region of the Se 3d and Na 2s photoemission lines (Al K_α excitation) of CuIn_{0.71}Ga_{0.29}Se₂ (CIGSe) samples exposed to ambient conditions for (a) <3 min, (b) 100 h, and (c) 1000 h and after different wet chemical surface treatments. Experimental data (open circles) are shown together with respective fits of the CIGSe component (blue line), a Cu_{2-x}Se component (green line), and the sum of both (red line). For the untreated “CIGSe 1000 h” sample an additional SeO₂ contribution is fitted. Voigt profiles together with a combined Shirley and linear background (black line below each detail spectrum) were used for the simultaneously performed fits. Below each spectrum the magnified residual (×3) of the fit is shown.

untreated CuIn_{0.71}Ga_{0.29}Se₂ that has been exposed to ambient air the longest duration investigated in this study (Fig. 6(c)). Furthermore, we observe a Na 2s signal for the untreated “CIGSe 100h” and “CIGSe 1000h” sample. The seeming contradiction that no Na 2s line can be identified for the untreated “CIGSe 3min” sample, while according to the Na 1s peak in Fig. 2, sodium present on all the untreated CuIn_{0.71}Ga_{0.29}Se₂ layer surfaces can be explained by the combination of low Na 1s intensity for the “CIGSe 3min” sample and the significantly lower photoionization cross section (σ) for the Na 2s line ($\sigma_{\text{Na } 1s} / \sigma_{\text{Na } 2s} \approx 20$ (Ref. 30)) and/or by the higher surface-sensitivity of the Na 1s measurement (the ratio of the inelastic mean free path of Na 1s photoelectrons to that of Na 2s photoelectrons is approximately $1/4$ ³¹). Both the sodium as well as the oxidized Se phase (and/or a Na-Se-O_x phase for the “CIGSe 1000h” sample) are completely removed by all applied wet-chemical surface treatments.

It has been reported previously⁶ that copper at the surface of chalcopyrite layers does not significantly oxidize unless the sample is exposed to air for an extended period of time. An oxidized copper phase can in principle be indicated by an asymmetric broadening towards higher binding energies of related photoemission peak—as discussed above for the Ga 2p_{3/2} and In 3d_{3/2} lines. However, the comparatively small energy separation of copper-related XPS peaks complicates the unambiguous identification of different copper species. Fig. 7 shows the Cu 2p_{3/2} photoelectron spectra for the studied CuIn_{0.71}Ga_{0.29}Se₂ layers as a function of air exposure and wet-chemical surface treatment. Close inspection of the data indeed reveals that the photoemission line is asymmetrically broadened towards higher binding

energies for the “CIGSe 100h” and “CIGSe 1000h” samples, most easily noticed for the untreated “CIGSe 1000h” sample in Fig. 7(c). Therefore, the Cu 2p_{3/2} lines are fitted by (at least) two Voigt functions. The main Cu 2p_{3/2} contribution at $E_B = (932.2 \pm 0.1)$ eV can be attributed to copper in a chemical chalcopyrite environment.^{2,20} For the samples after 100 h and 1000 h of air exposure, a second contribution needs to be considered to derive a reasonable fit. This Cu 2p_{3/2} contribution is located at $E_B = (932.9 \pm 0.1)$ eV and assigned to be indicative for the presence of Cu_{2-x}Se (Ref. 7) in agreement with the attribution of the second Se 3d contribution (see above discussion related to Fig. 6).

According to thermodynamic reference data,² a Cu_{2-x}Se phase can easily form in case of Cu-rich grown chalcopyrites. Cahen *et al.*,⁷ however, also found Cu_{2-x}Se phases at the surface of Cu-poor grown CuInSe₂ layers. They proposed that oxygen primarily reacts with In and therefore even at Cu-poor grown chalcopyrites, a surplus of Cu and Se forms at the surface which lead to the formation of Cu_{2-x}Se compounds. The formation of such a Cu_{2-x}Se phase is very typical for the interface between chalcopyrites and their native oxide layers and could be verified by several groups.^{2,6,7} Consequently, it seems legitimate to attribute the broadening of the Cu 2p_{3/2} and the Se 3d towards higher binding energies to the presence of Cu_{2-x}Se. Another confirmation for this interpretation is the fact that the second Cu 2p_{3/2} contribution can only be completely removed by the wet-chemical KCN treatment and not by any NH₃ treatment.²⁹

Note that for a reasonable fit of the Cu 2p_{3/2} spectrum of the CuIn_{0.71}Ga_{0.29}Se₂ layer that has been exposed to air for 1000 h, an additional (third) contribution needs to be considered. This third contribution is located at $E_B = (934.1 \pm 0.1)$

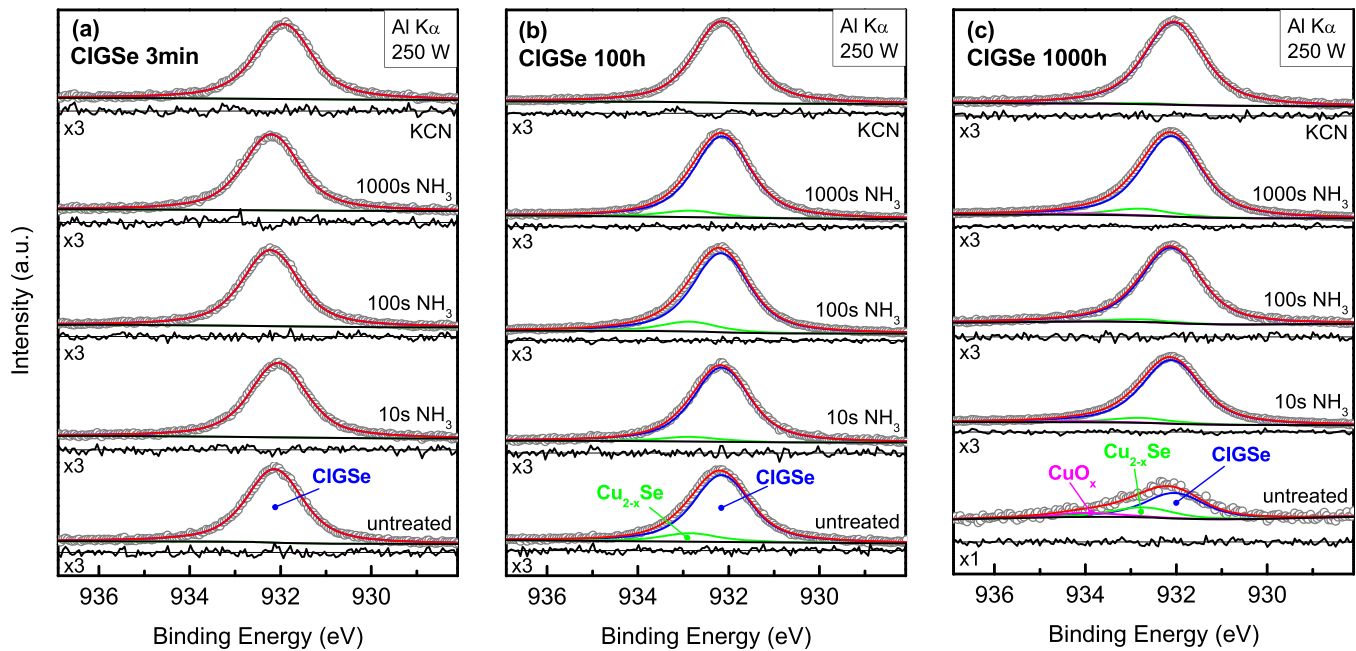


FIG. 7. Cu $2p_{3/2}$ photoemission spectra (Al K_{α} excitation) of $\text{CuIn}_{0.71}\text{Ga}_{0.29}\text{Se}_2$ (CIGSe) samples exposed to ambient conditions for (a) <3 min, (b) 100 h, and (c) 1000 h and after different wet chemical surface treatments. Experimental data (open circles) are shown together with respective fits of the CIGSe component (blue line), a Cu_{2-x}Se component (green line), a CuO_x component (magenta line), and the sum of all three fits (red line). Voigt profiles together with a combined Shirley and linear background (black line below each detail spectrum) were used for the simultaneously performed fits. Below each spectrum, the magnified residual ($\times 3$) of the fit is shown.

eV and can be assigned to a copper oxide (CuO_x) phase.³² As indicated in Fig. 7(c), all wet-chemical surface treatments are able to remove the CuO_x surface phase.

C. Oxide content

To allow for a more quantitative discussion, we calculated the partial oxide content C_X^{ox} of element X from the integrated intensities of the fitted photoemission lines as follows: $C_X^{\text{ox}} = \frac{I_{X(\text{oxide})}}{I_{X(\text{oxide})} + I_{X(\text{CIGSe})}}$, where $I_{X(\text{oxide})}$ ($I_{X(\text{CIGSe})}$) is the area of the fitted Voigt profile assigned to element X in the oxidized phase (CIGSe phase). Fig. 8 shows the calculated C_X^{ox} for $X = \text{Ga}, \text{In}, \text{Se},$ and Cu for the three air-exposure stages (“CIGSe 3 min,” “CIGSe 100 h,” “CIGSe 1000 h”) and as a function of the different chemical surface treatments, providing a direct comparison of the element-specific oxidation behavior. Note, however, that for this comparison, the impact of the different information depths of the analyzed photoemission lines was not taken into account.³³ Apparently, Ga is the element which is most susceptible to native oxidation. As a function of air exposure, $C_{\text{Ga}}^{\text{ox}}$ rises from $(10 \pm 1) \%$ for the “CIGSe 3 min” sample to $(49 \pm 24) \%$ for the “CIGSe 1000 h” sample. The removal of the oxide layer by wet-chemical means crucially depends on the duration of the treatment; the longer the $\text{CuIn}_{0.71}\text{Ga}_{0.29}\text{Se}_2$ layer is dipped into NH_3 solution the more Ga oxide is being removed from the surface. A complete removal of the Ga_2O_3 phase can only be achieved by 1000 s in NH_3 or the KCN treatment.

For indium, a detectable oxidation can only be identified for the “CIGSe 100 h” and “CIGSe 1000 h” samples. The fluctuation in $C_{\text{In}}^{\text{ox}}$ of the “CIGSe 3 min” sample is within the

error of the analysis procedure. For the “CIGSe 100 h,” it can be observed that the degree of surface oxidation is reduced with increasing wet-chemical surface treatment time. In contrast, the degree of oxidation of the “CIGSe 1000 h” sample is nearly unaffected by the wet-chemical treatment time. In this case, the In-oxide content remains constant with values between 20 and 25%, even after KCN treatment. This incomplete removal is likely due to the fact that In-oxides do not dissolve very well in the etching solutions³⁴ (in particular, compared to the other oxides found on an air-exposed chalcopyrite). The relatively low $C_{\text{In}}^{\text{ox}}$ of the untreated “CIGSe 1000 h” sample has to be viewed critically, in particular, since the untreated “CIGSe 100 h” and the 10 s NH_3 treated “CIGSe 1000 h” sample surfaces show a similar and a larger In-oxide content, respectively. We speculate that this disagreement is due to the formation of a passivating (gallium oxide) layer on the chalcopyrite surface preventing further indium oxidation and competing processes in the wet-chemical treatment solutions that lead to a preferred dissolution of the Ga-, Se-, and Cu-related oxides.

In agreement with the Auger and photoemission lines discussed above, for selenium and copper, the formation of a SeO_x -like [$C_{\text{Se}}^{\text{ox}} = (33 \pm 7) \%$] and a Cu-oxide [$C_{\text{Cu}}^{\text{ox}} = (14 \pm 3) \%$] phase is only observed for the 1000 h air-exposed $\text{CuIn}_{0.71}\text{Ga}_{0.29}\text{Se}_2$ samples. Both the Se- and Cu-based oxides can completely be removed by any of the treatments in aqueous NH_3 and KCN solutions.

Table I shows the standard formation enthalpies, ΔH_f^0 , given for oxides that might be found on an air-exposed $\text{CuIn}_{0.71}\text{Ga}_{0.29}\text{Se}_2$ absorber. In general, the oxidation tendencies indicated by the standard formation enthalpies are in very good agreement with the oxidation behavior derived

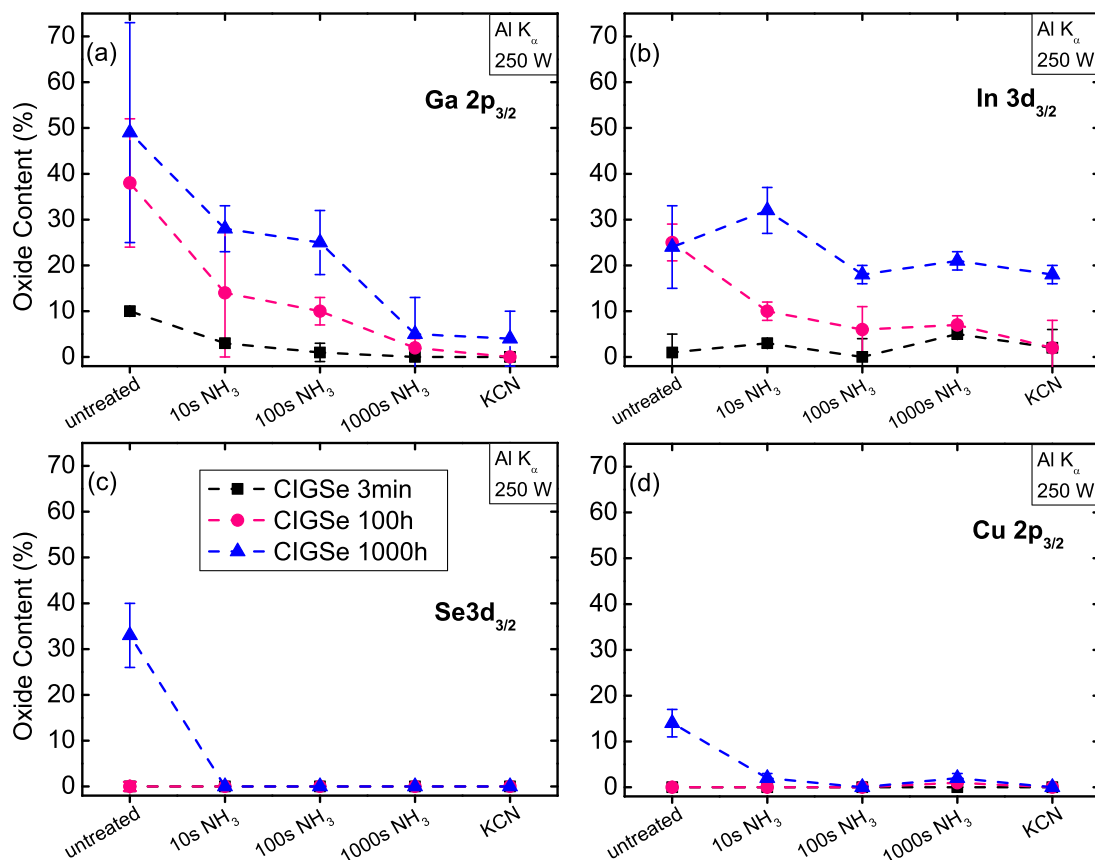


FIG. 8. XPS-derived elemental oxidation for different air-exposure times (<3 min, 100 h, and 1000 h) and their removal by wet-chemical treatments for (a) Ga, (b) In, (c) Se, and (d) Cu.

from the photoelectron spectra presented in our study and summarized in Fig. 8. Thus, from a purely thermodynamic point of view (under equilibrium conditions) and based on surface-sensitive XPS/XAES measurements, we tentatively find the prevalence of oxides formed on an air-exposed $\text{CuIn}_{0.71}\text{Ga}_{0.29}\text{Se}_2$ surface³³ to be in the order of Ga_2O_3 , In_2O_3 , SeO_x , and $\text{Cu}_2\text{O}/\text{CuO}$.

D. Influence of KCN treatment on oxide layer

Based on the presented analysis of the photoemission spectra, we find that the KCN treatment most effectively (and up to 100 h of air exposure also most reliably) removes natively formed surface oxides from $\text{CuIn}_{0.71}\text{Ga}_{0.29}\text{Se}_2$ surfaces and thus is the recommended first choice to clean chalcopyrites—even more so as it also removes Cu selenides. However, whether or not the KCN treatment additionally changes the chemical $\text{CuIn}_{0.71}\text{Ga}_{0.29}\text{Se}_2$ surface structure will be analyzed in the following. For a qualitative assessment, the photoelectron core-level spectra of Ga, In, Se, and

Cu of the untreated “CIGSe 3 min” sample are directly compared to the corresponding spectra of the KCN treated “CIGSe 100 h” sample in Fig. 9. For better illustration, the spectra were normalized. The normalization factor was chosen in such a way that the background on both sides of the peak is identical. Any difference in spectral shape indicating a varying presence of oxide or selenide phases will manifest itself in the respective difference spectra. From this, we find no indication for the presence of additional species on the surface of the 100 h air-exposed $\text{CuIn}_{0.71}\text{Ga}_{0.29}\text{Se}_2$ absorber after KCN treatment. In contrast, the only significant deviation from statistical noise can be seen in the difference spectra of the Ga 2p_{3/2} photoemission line that can be attributed to the presence of a Ga_2O_3 phase on the surface of the untreated $\text{CuIn}_{0.71}\text{Ga}_{0.29}\text{Se}_2$ sample that has been exposed to air for less than 3 min and that had been removed by the KCN treatment (see discussion related to Figs. 1 and 4).

To test whether the KCN treatment quantitatively impacts the chemical surface structure of the chalcopyrite absorber, the surface composition of the “CIGSe 3 min” and

TABLE I. Standard formation enthalpy ΔH_f^0 (at $T = 289\text{ K}$, 1 bar, in kJ/mol) of different Ga, In, Se, and Cu species that might form at the surface of a $\text{CuIn}_{0.71}\text{Ga}_{0.29}\text{Se}_2$ absorber.

Component	Ga_2O_3	In_2O_3	SeO_2	$\text{Cu}(\text{OH})_2$	Cu_2O	CuO	Cu_2Se	CuSe
ΔH_f^0 (Ref. 6)	-1089.1	/	-225.4	-449.8	-168.6	-157.3	-65.26	-39.5
ΔH_f^0 (Ref. 35)	-1089.1	-925.9	-225.1	/	-170.7	-156.1	-65.27	-41.8

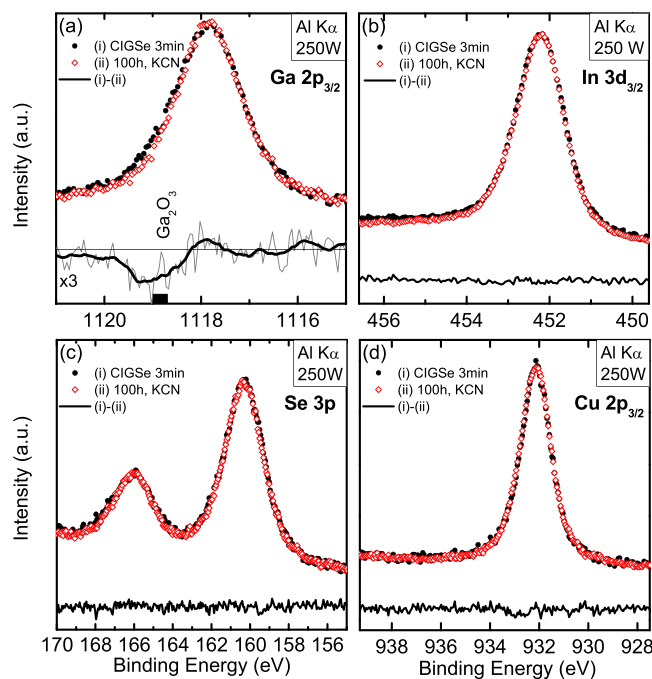


FIG. 9. Direct comparison of the (a) Ga $2p_{3/2}$, (b) In $3d_{3/2}$, (c), Se $3p$, and (d) Cu $2p_{3/2}$ XPS detail spectra (Al K_{α} excitation) of (i) the as-received “CIGSe 3 min” sample exposed to air for less than 3 min and of (ii) the KCN etched “CIGSe 100 h.” At the bottom of the panels, the magnified difference spectra (i)–(ii) are depicted. For the Ga $2p_{3/2}$ data, the reference position for Ga_2O_3 (Refs. 4 and 21) is indicated.

the KCN-treated “CIGSe 100 h” sample has been derived from the core level (Ga $2p_{3/2}$, In $3d_{3/2}$, and Cu $2p_{3/2}$) XPS data.³⁶ In addition, we used the XPS data collected using the two excitation sources (Mg K_{α} and Al K_{α}) to get some “depth-resolved” insights. Table II shows the calculated $[\text{In} + \text{Ga}]/[\text{Cu}]$ ratio for (a) the untreated and (b) the KCN treated $\text{CuIn}_{0.71}\text{Ga}_{0.29}\text{Se}_2$ layers that had been exposed to air for <3 min, 100 h, and 1000 h. The determined $(\text{Int}_{norm}^{\text{In}} + \text{Int}_{norm}^{\text{Ga}})/\text{Int}_{norm}^{\text{Cu}}$ ratio varies between 2.3 and 3.4, indicating a Cu depletion of the $\text{CuIn}_{0.71}\text{Ga}_{0.29}\text{Se}_2$ surface, which is characteristic for Cu-poor grown high-efficiency chalcopyrites.^{2,8,37–41} The differences and uncertainties in the derived $[\text{In} + \text{Ga}]/[\text{Cu}]$ ratios cloak potential trends. However, the fact that we generally find that the $[\text{In} + \text{Ga}]/[\text{Cu}]$ ratio after KCN treatment is lower compared to the chemical surface structure of the untreated $\text{CuIn}_{0.71}\text{Ga}_{0.29}\text{Se}_2$ layers might indicate some KCN-induced modification of the chalcopyrite surface composition in general and of the degree of Cu surface deficiency in particular.

TABLE II. $[\text{In} + \text{Ga}]/[\text{Cu}]$ surface composition of (a) the untreated and (b) the KCN treated $\text{CuIn}_{0.71}\text{Ga}_{0.29}\text{Se}_2$ layer for different air-exposure times, calculated from the core level XPS data probed with Al K_{α} and Mg K_{α} excitation. The experimental uncertainty is ± 0.3 for (a) and ± 0.2 for (b).

$[\text{In} + \text{Ga}]/[\text{Cu}]$	CIGSe 3 min		CIGSe 100 h		CIGSe 1000 h	
	Mg K_{α}	Al K_{α}	Mg K_{α}	Al K_{α}	Mg K_{α}	Al K_{α}
(a) Untreated	3.2	3.0	2.9	3.0	-	3.4
(b) KCN	2.8	2.9	2.3	2.9	2.8	2.8

As a result, we find that the KCN treatment removes native oxides creating a chemical $\text{CuIn}_{0.71}\text{Ga}_{0.29}\text{Se}_2$ surface structure that is almost identical to the surface of the untreated “CIGSe 3 min” sample, if the air-exposure time is limited to below 100 h.

IV. CONCLUSIONS

We systematically analyzed the oxidation behavior and the influence of wet chemical surface treatments on polycrystalline $\text{CuIn}_{0.71}\text{Ga}_{0.29}\text{Se}_2$ layers under defined ambient conditions. For this purpose, $\text{CuIn}_{0.71}\text{Ga}_{0.29}\text{Se}_2$ layers were exposed to air for <3 min, 100 h, or 1000 h, treated with KCN- or NH_3 -based aqueous solutions, and analyzed using surface sensitive x-ray photoelectron and x-ray excited Auger electron spectroscopy. Quantitative analysis of the photoemission spectra revealed that oxygen primarily reacts with Ga and In. This behavior is well reflected by the thermodynamic reference data (standard formation enthalpies) of related oxide compounds. Furthermore, the segregation of Cu selenides at the surface of the chalcopyrite could be verified in agreement with literature.^{2,7,15} This selenide phase can be removed by KCN solution which was confirmed to be the best surface treatment to produce defined and reproducible chemical surface conditions. We could show that the KCN treated surface of air-exposed $\text{CuIn}_{0.71}\text{Ga}_{0.29}\text{Se}_2$ layers is in its chemical surface structure – apart from a slight change in surface composition (i.e., Cu deficiency) – identical to a (nearly) non air-exposed surface if exposure is limited to 100 h. This finding is not only crucial for the reliable/reproducible employment of surface science tools to study chalcopyrite surfaces but also needs to be considered for solar cell production in the laboratory and in an industrial mass-production environment.

ACKNOWLEDGMENTS

The authors gratefully acknowledge financial support from the Bundesministerium für Umwelt, Naturschutz und Reaktorsicherheit (BMU) under Contract No. 0327559H. M.B. acknowledges financial support by the Helmholtz-Association (VH-NG-423) and D. Fuertes Marrón is gratefully acknowledged for stimulating discussions.

¹ZSW press release (22 September 2014), <http://www.zsw-bw.de/uploads/media/pr12-2014-ZSW-WorldrecordCIGS.pdf>.

²D. Schmid, M. Ruckh, and H.-W. Schock, *Appl. Surf. Sci.* **103**, 409 (1996).

³Y. Hashimoto, N. Kohara, T. Negami, M. Nishitani, and T. Wada, *Jpn. J. Appl. Phys. Part 1* **35**, 4760 (1996).

⁴H. Iwakuro, C. Tatsuyama, and S. Ichimura, *Jpn. J. Appl. Phys. Part 1* **21**, 94 (1982).

⁵C. Heske, D. Eich, R. Fink, E. Umbach, T. van Buuren, C. Bostedt, S. Kakar, L. J. Terminello, M. M. Grush, T. A. Callcott, F. J. Himpsel, D. L. Ederer, R. C. C. Perera, W. Riedl, and F. Karg, *Surf. Interface Anal.* **30**, 459 (2000).

⁶R. Wuerz, A. Meeder, D. Fuertes Marrón, and T. Schedel-Niedrig, *Phys. Rev. B* **70**, 205321 (2004).

⁷D. Cahen, P. J. Ireland, L. L. Kazmerski, and F. A. Thiel, *J. Appl. Phys.* **57**, 4761 (1985).

⁸M. Bär, I. Repins, M. Contreras, L. Weinhardt, R. Noufi, and C. Heske, *Appl. Phys. Lett.* **95**, 052106 (2009).

⁹M. Bär, J. Klaer, L. Weinhardt, R. G. Wilks, S. Krause, M. Blum, W. Yang, C. Heske, and H.-W. Schock, *Adv. Energy Mater.* **3**, 777 (2013).

- ¹⁰S. Sadewasser, T. Glatzel, S. Schuler, S. Nishiwaki, R. Kaigawa, and M. Lux-Steiner, *Thin Solid Films* **431–432**, 257 (2003).
- ¹¹C.-S. Jiang, F. Hasoon, H. Moutinho, H. Al-Thani, M. Romero, and M. Al-Jassim, *Appl. Phys. Lett.* **82**, 127 (2003).
- ¹²M. J. Romero, C.-S. Jiang, R. Noufi, and M. Al-Jassim, *Appl. Phys. Lett.* **87**, 172106 (2005).
- ¹³S. Sadewasser, *Phys. Status Solidi A* **203**, 2571 (2006).
- ¹⁴H. Mönig, Y. Smith, R. Caballero, C. A. Kaufmann, I. Laueremann, M. C. Lux-Steiner, and S. Sadewasser, *Phys. Rev. Lett.* **105**, 116802 (2010).
- ¹⁵L. L. Kazmerski, O. Jamjoum, P. J. Ireland, S. K. Deb, R. A. Mickelsen, and W. Chen, *J. Vac. Sci. Technol.* **19**, 467 (1981).
- ¹⁶L. C. Olsen, F. W. Addis, L. Huang, W. N. Shafarman, P. Eschbach, and G. J. Exarhos, in *Conference Record of the 28th IEEE Photovoltaic Specialists Conference*, Piscataway, NJ (IEEE, 2000), p. 458.
- ¹⁷C. A. Kaufmann, A. Neisser, R. Klenk, and R. Scheer, *Thin Solid Films* **480–481**, 515 (2005).
- ¹⁸C. A. Kaufmann, R. Caballero, T. Unold, R. Hesse, R. Klenk, S. Schorr, M. Nichterwitz, and H.-W. Schock, *Sol. Energy Mater. Sol. Cells* **93**, 859 (2009).
- ¹⁹M. P. Seah, *Surf. Interface Anal.* **14**, 488 (1989).
- ²⁰A. Klyner, *J. Electrochem. Soc.* **146**, 1816 (1999).
- ²¹G. Schön, *J. Electron Spectrosc. Relat. Phenom.* **2**, 75 (1973).
- ²²P. A. Bertrand, *J. Vac. Sci. Technol.* **18**, 28 (1981).
- ²³C. Wagner and P. Biloen, *Surf. Sci.* **35**, 82 (1973).
- ²⁴M. Ruckh, D. Schmid, M. Kaiser, R. Schäffler, T. Walter, and H.-W. Schock, *Sol. Energy Mater. Sol. Cells* **41–42**, 335 (1996).
- ²⁵D. W. Niles, K. Ramanathan, F. Hasoon, R. Noufi, B. J. Tielsch, and J. E. Fulghum, *J. Vac. Sci. Technol. A* **15**, 3044 (1997).
- ²⁶C. Heske, G. Richter, Z. Chen, R. Fink, E. Umbach, W. Riedl, and F. Karg, *J. Appl. Phys.* **82**, 2411 (1997).
- ²⁷C. D. Wagner, L. H. Gale, and R. H. Raymond, *Anal. Chem.* **51**, 466 (1979).
- ²⁸C. D. Wagner, *Discuss. Faraday Soc.* **60**, 291 (1975).
- ²⁹Note that while selenium oxides are soluble in water and hence should be removed by both, the aqueous NH_3 as well as the aqueous KCN solution, copper selenides are only soluble in a KCN solution.
- ³⁰J. H. Scofield, *J. Electron Spectrosc. Relat. Phenom.* **8**, 129 (1976).
- ³¹QUASES-IMFP-TPP2M software (<http://www.quases.com>) applying the TPP2M algorithm described in S. Tanuma, C. J. Powell, and D. R. Penn, *Surf. Interface Anal.* **21**, 165 (1994).
- ³²N. S. McIntyre and M. G. Cook, *Anal. Chem.* **47**, 2208 (1975).
- ³³As the kinetic energy here considered photoelectrons' changes from ≈ 369 eV for Ga $2p_{3/2}$, over ≈ 555 eV for Cu $2p_{3/2}$ and ≈ 1035 eV for In $3d_{3/2}$ to ≈ 1432 eV for Se $3d_{5/2}$, the inelastic mean free path (IMFP) in a stoichiometric chalcopyrite absorber probed with Al K_{α} excitation increases: IMFP (Ga $2p_{3/2}$) ≈ 1.2 nm < IMFP (Cu $2p_{3/2}$) ≈ 1.6 nm < IMFP (In $3d_{3/2}$) ≈ 2.6 nm < IMFP (Se $3d_{5/2}$) ≈ 3.4 nm (IMFPs calculated according to Ref. 31). In consequence, the information depth of the Ga $2p_{3/2}$, Cu $2p_{3/2}$, In $3d_{3/2}$, and Se $3d_{5/2}$ core levels is different and thus might influence the derived oxidation prevalence. However, as the prevalence of oxides formed on an air-exposed $\text{CuIn}_{0.71}\text{Ga}_{0.29}\text{Se}_2$ surface was derived to be in the order of Ga_2O_3 , In_2O_3 , Se-O_x , and $\text{Cu}_2\text{O/CuO}$, the impact of the information depth can, however, not be dominant.
- ³⁴A. F. Holleman and E. Wiberg, in *Lehrbuch der anorganischen Chemie*, edited by E. Wiberg (Walter de Gruyter & Co, 1971).
- ³⁵O. Knacke and O. Kubaschewski, in *Thermochemical Properties of Inorganic Substances*, edited by K. Hesselmann (Springer, Heidelberg, 1991).
- ³⁶By normalization of the intensities of the photoelectron spectra, it is possible to gain information about the surface composition. Assuming a homogeneous distribution of the element concentration, the normalized intensity can be derived from

$$\text{Int}_{\text{norm}}^X = \frac{\text{Int}_{\text{det}}^X}{\lambda^{\text{CIGSe}}(E_{\text{kin}}) \cdot \frac{d\sigma^X}{\Omega(h\nu)} \cdot T(E_{\text{kin}}) \cdot Z}$$

where $\text{Int}_{\text{norm}}^X$ is the normalized intensity of a spectral line X, $\text{Int}_{\text{det}}^X$ the intensity of the same line measured by the detector, $\lambda^{\text{CIGSe}}(E_{\text{kin}})$ the inelastic mean free path for photoelectrons in $\text{CuIn}_{0.71}\text{Ga}_{0.29}\text{Se}_2$ with energy E_{kin} ,³¹ $\frac{d\sigma^X}{\Omega(h\nu)}$ the partial photoionization cross section of spectral line X with excitation energy $h\nu$,³⁰ $T(E_{\text{kin}})$ the transmission function of the analyzer for electrons with energy E_{kin} , and Z the number of scans. The transmission function was determined according to the survey spectra approach by recording a gold spectrum and adjusting it with a reference spectrum [M. P. Seah and G. C. Smith, *Surf. Interface Anal.* **15**, 751 (1990); G. C. Smith and M. P. Seah, *ibid.* **16**, 144 (1990)].

³⁷J. R. Tuttle, D. S. Albin, and R. Noufi, *Sol. Cells* **30**, 21 (1991).

³⁸D. Schmid, M. Ruckh, F. Grunwald, and H.-W. Schock, *J. Appl. Phys.* **73**, 2902 (1993).

³⁹D. Liao and A. Rockett, *Appl. Phys. Lett.* **82**, 2829 (2003).

⁴⁰H. Mönig, Ch.-H. Fischer, R. Caballero, Ch. A. Kaufmann, N. Allsop, M. Gorgoi, R. Klenk, H.-W. Schock, S. Lehmann, M. C. Lux-Steiner, and I. Laueremann, *Acta Mater.* **57**, 3645 (2009).

⁴¹X. Song, R. Caballero, R. Félix, D. Gerlach, C. A. Kaufmann, H.-W. Schock, R. G. Wilks, and M. Bär, *J. Appl. Phys.* **111**, 034903 (2012).